

Synthesis of ultrafine zeolites by dry-gel conversion without any organic additive

D. Hu^a, Q.-H. Xia^{a,*}, X.-H. Lu^a, X.-B. Luo^a, Z.-M. Liu^b

^a Ministry-of-Education Key Laboratory for the Synthesis and Application of Organic Functional Molecules & School of Chemistry and Chemical Engineering, Hubei University, 11 Xueyuan Road, Wuchang District, Wuhan 430062, China

^b Group 803, Dalian Institute of Chemical Physics of Chinese Academy of Sciences, Dalian 116023, China

Received 14 August 2007; received in revised form 17 December 2007; accepted 16 January 2008

Available online 20 January 2008

Abstract

ZSM-5, mordenite, cancrinite and Y zeolites were successfully crystallized by the dry-gel conversion (DGC) without any organic additive (or template), in which the crystal particles of ZSM-5, mordenite and Y zeolite were well controlled in the range of ultrafine size. With a molar ratio of $\text{SiO}_2/\text{Al}_2\text{O}_3 \leq 40$, the pure ZSM-5 zeolite was obtained at 170 °C at the $\text{Na}_2\text{O}/\text{SiO}_2$ molar ratio < 0.2 , but the pure mordenite was formed at 150 °C at the $\text{Na}_2\text{O}/\text{SiO}_2$ molar ratio > 0.25 . When the dry-gel with a composition of $5.0\text{Na}_2\text{O}:\text{Al}_2\text{O}_3:5.0\text{SiO}_2$ was crystallized at 140 °C for 24 h, pure cancrinite phase was obtained. TEM images showed that thus-crystallized zeolites consisted of ultrafine particles ranging 35–150 nm for ZSM-5, 50–200 nm for mordenite and 120–200 nm for zeolite Y, respectively. Different from ZSM-5, mordenite and cancrinite zeolites, the DGC synthesis of Y zeolite required more water in the dry-gel before crystallization.

© 2008 Elsevier Ltd. All rights reserved.

Keywords: A. Inorganic compounds; A. Microporous materials; A. Nanostructures; B. Chemical synthesis; B. Crystal growth

1. Introduction

Molecular sieves are an important class of materials that are widely used in a number of industries, e.g. large-scale applications as cracking catalysts in the oil industry and as water softening additives for detergents. These porous materials are becoming more important in the synthesis of bulk and fine chemicals where they offer an environmentally benign alternative to corrosive liquid acids and oxidants. Also, separation technologies make use of molecular sieves, and some interests are triggered because of their molecular recognition and nanochemical host possibilities.

Zeolites were first synthesized in 1862 [1]. Since then, numerous methods have been developed to synthesize zeolites and zeolite-like molecular sieves, in which the hydrothermal synthesis is almost an exclusively common route. In 1990, Xu et al. [2] reported that a dry aluminosilicate gel could be transformed to MFI by assistance with vapors of water and volatile amines, which is called dry-gel conversion (DGC). Since then, the DGC method has extensively been employed to synthesize microporous crystals and membranes with new compositions and structures [3].

* Corresponding author. Tel.: +86 27 50865370; fax: +86 27 50865370.

E-mail address: xia1965@yahoo.com (Q.H. Xia).

Mass transfer limitation plays an important role in industrial applications of zeolites. However, zeolites with small size are important in catalytic and adsorptive applications, and smaller crystals of zeolites will have larger surface areas and less diffusion limitations [4]. Nanosized zeolites also offer advantages in supramolecular catalysis, photochemistry, nanochemistry, electrochemistry, and optoelectronics, etc. [5]. Zeolite nanocrystals can also be used in the construction of other geometries such as thin films, fibers, and self-standing zeolite membranes, etc. [6]. Syntheses of nanosized or ultrafine particles of zeolite A, Y, silicalite, sodalite, ZSM-5, zeolite L, and zeolite beta were previously reported [4–7]. Morденite crystallites in the size range of 80–120 nm were also synthesized by hydrothermal transformation of Na-magadiite or by modification of different synthetic parameters [8,9]. Several reports have shown the DGC synthesis of nanosized or ultrafine zeolites with large BET surface areas and high activity in the presence of organic templates, in which one two-step temperature program was applied, where lower temperature was beneficial to the nucleation, and subsequent higher temperature could promote the growth of crystals [10–12]. Advantages of the DGC route lie in the physical separation of dry-gel with water to increase the yield of solid products, the reduction of organic template amount to decrease the cost and pollution, the variation of mass transfer during the crystallization to limit the crystal size and to increase the catalytic activity, etc.

However, to date, no report has approached the synthesis of zeolites with ultrafine particles by the DGC without the assistance of any organic additive. The present study first reports the DGC synthesis of ultrafine zeolites like ZSM-5, mordenite and Y without any organic additive (or template). And, the effects of crystallization conditions like reaction time, reaction temperature, water amount, $\text{SiO}_2/\text{Al}_2\text{O}_3$ and $\text{Na}_2\text{O}/\text{SiO}_2$ molar ratios were further revealed.

2. Experimental

2.1. Materials

The used materials included aerosil-200 (99% silica, degussa), sodium aluminate (AR, 84.23% alumina), sodium hydroxide (AR, 96%) and deionized water.

2.2. Synthesis of zeolite samples

Generally, an appropriate amount of sodium aluminate and sodium hydroxide was dissolved into a certain amount of deionized water to form a transparent solution, and then was added with 2.0 g of aerosil-200 silica powder. The resulting mixture was stirred at room temperature for about 30 min to obtain a homogeneous hydrogel. This gel was dried at 80 °C for 7 h to form a dry-gel, which was then ground into a fine powder with a uniform composition of $x\text{Na}_2\text{O}:\text{Al}_2\text{O}_3:y\text{SiO}_2$. About 0.3–0.8 g of amorphous dry-gel powder was placed in a Teflon beaker and transferred into a Teflon-lined stainless-steel autoclave (100 ml), in which about 9–12 g of water was poured into the bottom, and the fine powder gel was physically separated from water [10]. The autoclave was sealed and heated at desired temperatures in the oven for some time under autogenous pressure. After the completion of crystallization, the autoclave was quenched with tap water and the recovered solid product was washed several times with deionized water of about 400 ml, followed by drying at 80 °C overnight.

2.3. Characterization

X-ray diffraction (XRD) analysis was carried out using a Rigaku D/MAX IIIC diffractometer with $\text{Cu K}\alpha$ radiation operating at 30 kV and 25 mA. The relative crystallinity was evaluated by comparing the area of the characteristic peaks of the solid product with that of the reference zeolite sample synthesized by conventional method. Autosorb-1 was used to determine BET surface areas of zeolite products (calcined) obtained by present routes. Infrared spectral data were recorded on a Shimadzu IR Prestige-21 Fourier Transform Infrared Spectrophotometer; the samples were ground with KBr and pressed into thin wafers. Thermogravimetric and differential thermal analysis (TG/DTA) analyses were conducted by a Shimadzu DTG-60 thermogravimetric analyzer. The samples were heated in air from ambient temperature to 1000 °C at a heating rate of 10 °C/min. The morphology of crystalline materials was observed on a Nippon Electronics JEM-100SX transmission electron microscope (TEM); the particle sizes of samples were accordingly calculated based on TEM images. The $\text{SiO}_2/\text{Al}_2\text{O}_3$ ratios of zeolite products were measured by chemical analysis.

3. Results and discussion

3.1. Synthesis of ultrafine ZSM-5 and mordenite by DGC route

As one can see from Table 1, the initial $\text{Na}_2\text{O}/\text{SiO}_2$ and $\text{SiO}_2/\text{Al}_2\text{O}_3$ molar ratios strongly affected the formation of zeolite phases. Pure ZSM-5 phase could be achieved at 170 °C as the $\text{SiO}_2/\text{Al}_2\text{O}_3$ molar ratio was not higher than 30 with a molar ratio of $\text{Na}_2\text{O}/\text{SiO}_2 < 0.2$, while the molar ratios of $\text{Na}_2\text{O}/\text{SiO}_2 > 0.2$ led to a competition between ZSM-5 and mordenite phase (in the range of 150–170 °C). Under the present conditions, 0.2 of $\text{Na}_2\text{O}/\text{SiO}_2$ molar ratio seemed to be a critical value for inducing pure ZSM-5 phase. Pure mordenite phase was synthesized from 140 to 170 °C in the range of both the $\text{Na}_2\text{O}/\text{SiO}_2$ ratio from 0.3 to 0.375 and the $\text{SiO}_2/\text{Al}_2\text{O}_3$ ratio from 10 to 40. When the $\text{SiO}_2/\text{Al}_2\text{O}_3$ ratio was decreased to 10, 0.55 of $\text{Na}_2\text{O}/\text{SiO}_2$ molar ratio resulted in the intergrowth of NaP_1 + zeolite Y at 100 °C. Along with a continuous reduction of the $\text{SiO}_2/\text{Al}_2\text{O}_3$ ratio to 5 and an increase of the $\text{Na}_2\text{O}/\text{SiO}_2$ ratio to 1.0, zeolite cancrinite (CAN) and Y always co-existed in the temperature range from 100 to 120 °C. However, while increasing the crystallization temperature to 140 °C one pure CAN zeolite phase was achieved in 24 h. It is noteworthy that using the same procedure as stated above one pure Y zeolite phase could not be obtained whatever the crystallization parameters were varied.

The relative crystallinity of three ZSM-5 products was changed from 73% to 92% with variable BET surface areas from 346.4 to 387.1 m^2/g . Very distinctly the respective $\text{SiO}_2/\text{Al}_2\text{O}_3$ molar ratios of three ZSM-5 samples were 20.3, 21.5 and 29.4, considerably close to the dry-gel compositions, notably different from the cases of mordenite zeolites. For the latter, the $\text{SiO}_2/\text{Al}_2\text{O}_3$ molar ratios of three products were 9.8, 13.3 and 15.9, appreciably lower than those in dry-gels. This means the difficulty in achieving mordenite zeolites with high $\text{SiO}_2/\text{Al}_2\text{O}_3$ ratios by the DGC route. With the variation of the $\text{SiO}_2/\text{Al}_2\text{O}_3$ ratio in the dry-gel, the relative crystallinity of mordenite products was changed from 34% to 91%, in which BET surface areas of three products ranged from 470.2 to 513.4 m^2/g .

Fig. 1 presents the XRD patterns of ZSM-5 crystallized at 170 °C from the dry-gel with a composition of $3.8\text{Na}_2\text{O}:\text{Al}_2\text{O}_3:30\text{SiO}_2$. Obviously, within 24 h the ZSM-5 framework just began to form; within 48 h the solid product exhibited typical of MFI characteristics with diffraction peaks at 7.86° , 8.78° , 23.10° , 23.78° , 24.38° , 29.91° , 44.94° and 45.57° 2θ , indexed to (0 1 1), (0 2 0), (0 5 1), (5 1 1), (-3 1 3), (0 5 3), (0 1 0 0) and (1 0 0 0) miller indices. Along with the increase of the crystallization time to 72 h, the crystallinity was notably enhanced. IR vibrations of the framework clearly appeared at 1222, 1095, 802, 549 and 460 cm^{-1} , in which the peak at 549 cm^{-1} is the fingerprint vibration of 5-membered-ring apertures of pentasil zeolite. TG/DTA curves of typically thus-prepared ZSM-5 sample were determined in order to evaluate the weight loss behaviors of the samples synthesized by the DGC

Table 1
Effect of reaction conditions (reaction time, temperature, $\text{SiO}_2/\text{Al}_2\text{O}_3$ and $\text{Na}_2\text{O}/\text{SiO}_2$) on the crystalline phase

Entry	Time (h)	Temperature (°C)	Gel $\text{Na}_2\text{O}/\text{SiO}_2$	Gel $\text{SiO}_2/\text{Al}_2\text{O}_3$	Product $\text{SiO}_2/\text{Al}_2\text{O}_3$	Relative crystallinity (%)	BET surface area (m^2/g)	Phase
1	72	170	0.05	60				Amorphous
2	72	170	0.075	60				ZSM-5 + unknown
3	72	170	0.127	30	29.4	78	346.4	ZSM-5
4	72	170	0.175	20	21.5	80	365.5	ZSM-5
5	72	170	0.2	20	20.3	92	387.1	ZSM-5
6	72	150	0.2	30				Mordenite + ZSM-5
7	24	170	0.2	30				Mordenite + ZSM-5
8	72	140	0.375	40		34		Mordenite
9	24	150	0.3	20	13.3	91	513.4	Mordenite
10	24	160	0.32	10	9.8	62	470.2	Mordenite
11	48	170	0.33	30	15.9	73	479.6	Mordenite
12	10–24	90–100	0.5–0.55	10				NaP_1 + Y
13	24	100–120	1.0	5				CAN + Y
14	24	140	1.0	5				CAN
15 ^a	6/18	50/90	1.0	5				Unknown
16 ^a	6/18	50/90	1.0	5	4.5	80	822.4	Y

^a Two-step temperature program. The $\text{H}_2\text{O}/\text{SiO}_2$ molar ratio in the dry-gel was ca. 1.33 for entry 15, ca. 2.0 for entry 16, and ca. 0.66 for other entries.

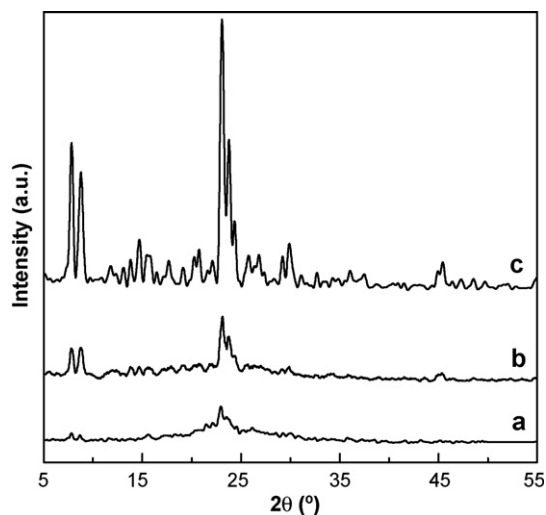


Fig. 1. Effect of time on XRD patterns of ZSM-5 crystallized at 170 °C from the dry-gel with a composition of 3.8Na₂O:Al₂O₃:30SiO₂. (a) 24 h, (b) 48 h and (c) 72 h.

route. As depicted in Fig. 2, the TG curve of the sample showed only one-stage weight loss in the flow of air, without any weight loss of organic template by combustion. Apparently, the weight loss (9.8 wt.%) below 300 °C accompanied with an endothermic peak was due to the desorption of physically adsorbed water and other small molecules inside channels. A weak exothermic DTA signal was observed to locate at about 836 °C, ascribable to the collapse of MFI structure, because there was not any weight loss at this temperature on its TG curve, and the sample calcined at 850–900 °C became amorphous (checked by XRD) with low BET surface areas of 64.5–87.3 m²/g.

XRD patterns of mordenite crystallized at 150 °C from the dry-gel with a composition of 6Na₂O:Al₂O₃:20SiO₂ were shown in Fig. 3. No diffraction peak was observed within 16 h, meaning that the crystallization did not occur at all. As the crystallization time was increased to 24 h, some strong characteristic diffractions emerged at 6.58°, 9.86°, 13.50°, 19.68°, 22.32°, 25.76°, 26.32°, 27.92°, 30.94° and 35.72° 2θ, typical of MOR lattice, without appreciable amorphous phase, indicating the complete crystallization of mordenite zeolite by the DGC route. Along with

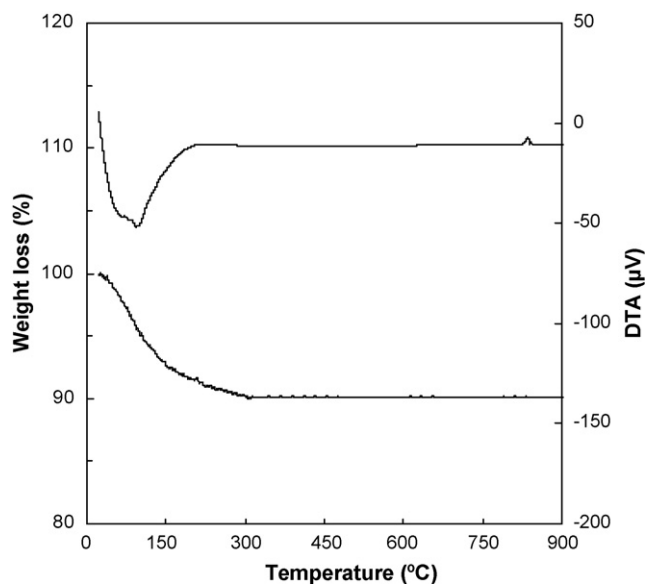


Fig. 2. TG-DTA curves of typical ZSM-5 sample synthesized by DGC route without any organic additive.

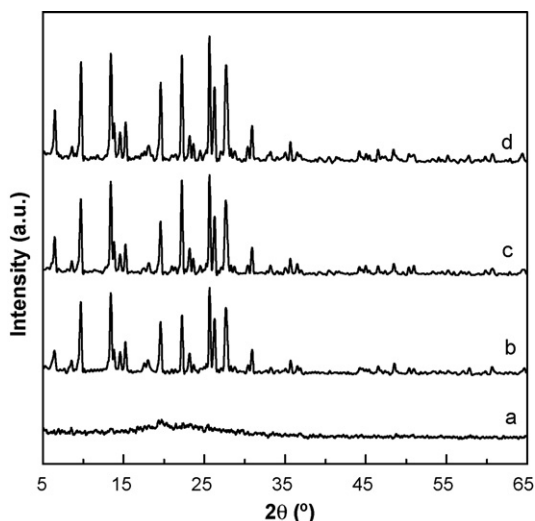


Fig. 3. Effect of time on XRD patterns of mordenite crystallized at 150 °C from the dry-gel with a composition of 6Na₂O:Al₂O₃:20SiO₂. (a) 16 h, (b) 24 h, (c) 36 h and (d) 48 h.

prolonging the time to 48 h, the crystallinity was further increased. IR vibrations of the framework emerged at 1225, 1050, 800, 720, 580, 560 and 450 cm⁻¹, in which two peaks at 580 and 560 cm⁻¹ are characteristic vibrations of double-ring apertures of MOR zeolite [13].

Fig. 4 illustrates TEM micrographs of ZSM-5 and mordenite samples crystallized by the DGC. For the ZSM-5 sample achieved at 170 °C, the morphology was mainly consisted of spherical ultrafine crystallites with the size of 35–150 nm (in Fig. 4a and b). However, for the ZSM-5 sample crystallized at 180 °C, a small increase of temperature led to the formation of larger aggregates with an increased size of 70–230 nm (still in the range of ultrafine size) packed by nanosized particles (in Fig. 4c and d). This means that the growth of ZSM-5 crystals could be promoted by the increase of temperature under the present conditions. Although mordenite zeolite was crystallized at a lower temperature of 150 °C, the size of spherical crystals reached 50–200 nm (in Fig. 4e and f), obviously larger than 35–150 nm of the ZSM-5 zeolite, indicating the easy aggregation of mordenite crystals under DGC conditions.

3.2. Synthesis of ultrafine Y zeolite by the DGC route

As shown in Table 1, when the molar composition of dry-gel was 5.0–5.5Na₂O:Al₂O₃:10SiO₂, the resulting solid was always a mixed phase of NaP₁ + Y at 100 °C for 10–24 h. However, when the composition of dry-gel was changed to 5.0Na₂O:Al₂O₃:5.0SiO₂, i.e. the amount of alumina was doubled in the dry-gel, the recovered solid was consisted of Y + CAN in the range of 100–120 °C. In this case, even though more water was pre-added into the dry-gel, still a mixed phase of CAN + Y was obtained. But, when the dry-gel with a composition of 5.0Na₂O:Al₂O₃:5.0SiO₂ was crystallized at 140 °C for 24 h, one pure CAN phase was obtained. Fig. 5 compares XRD patterns of cancrinite + Y and pure cancrinite zeolites crystallized from the dry-gel with a composition of 5Na₂O:Al₂O₃:5SiO₂. Clearly, the XRD pattern in Fig. 5d does not contain any impurity phase, which is a standard diffraction profile of pure cancrinite zeolite (typical of CAN topology) with some diffractions of 13.97°, 19.32°, 24.63°, 27.62°, 33.10°, 35.0°, 35.27°, 37.73° and 43.30° 2θ.

The samples 15 and 16 in Table 1 with a composition of 5Na₂O:Al₂O₃:5SiO₂ was crystallized by one two-step temperature program, in which the crystallization was carried out at 50 °C for 6 h and subsequently at 90 °C for 18 h. Different from the DGC crystallization of ZSM-5, mordenite and cancrinite zeolites (ca. 0.66 of the H₂O/SiO₂ ratio in the dry-gel), the DGC synthesis of Y zeolite required more water in the dry-gel before crystallization, e.g. the H₂O/SiO₂ molar ratio in the dry-gel was ca. 1.33 for entry 15 and ca. 2.0 for entry 16. However, it must be noticed that 1.33–2.0 of the H₂O/SiO₂ ratio in the dry-gel was still much lower than 10–20 used in traditional hydrothermal conversion (HTC). This showed the nucleation and growth of Y zeolite crystals under DGC conditions needed the assistance of more water than those of ZSM-5, mordenite and cancrinite zeolites. Fig. 6 compares XRD patterns of two samples 15

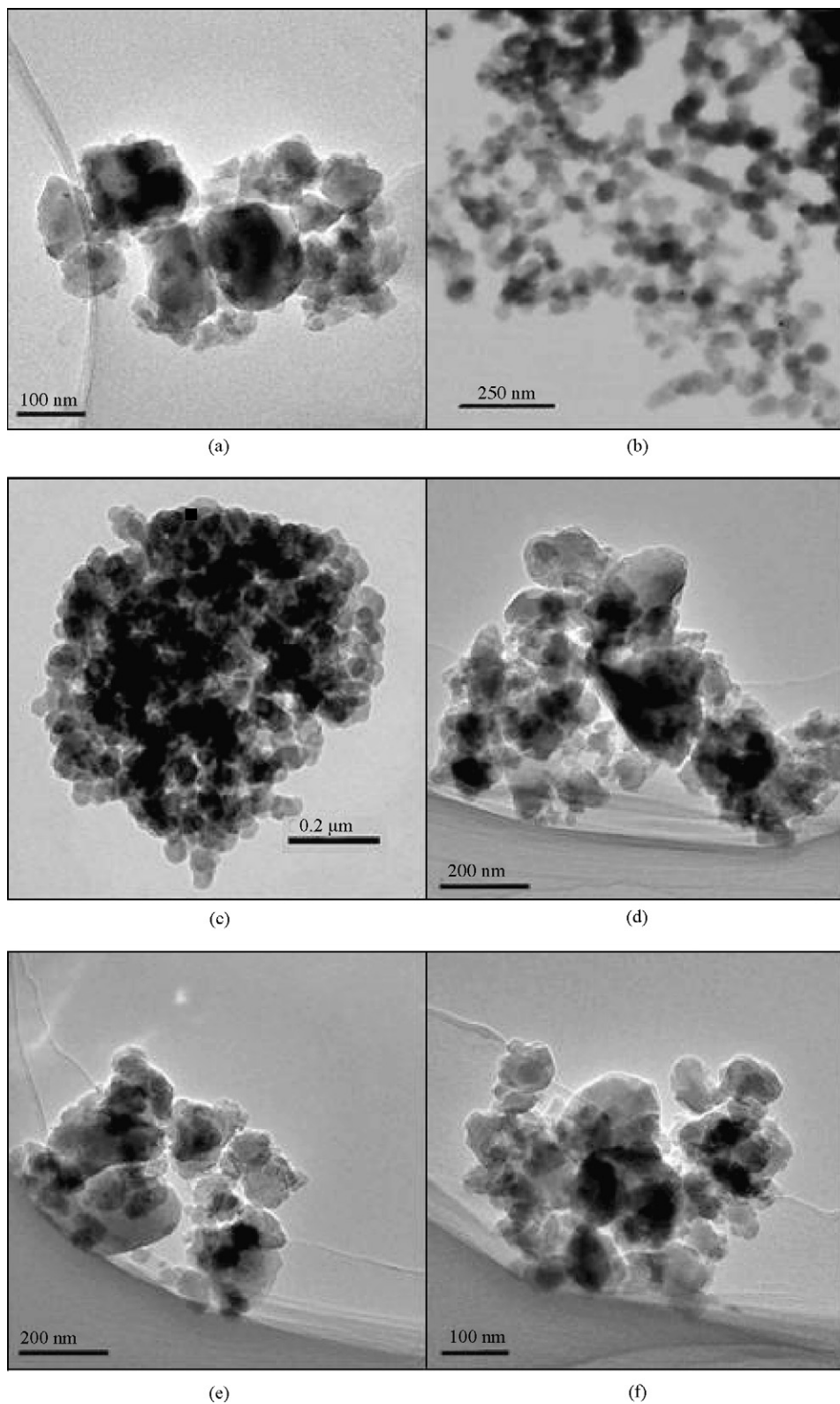


Fig. 4. TEM images of zeolites ZSM-5 and mordenite synthesized by dry-gel conversion (ZSM-5: (a) and (b) 170 °C for 72 h, (c) and (d) 180 °C for 72 h; mordenite: (e) and (f) 150 °C for 72 h).

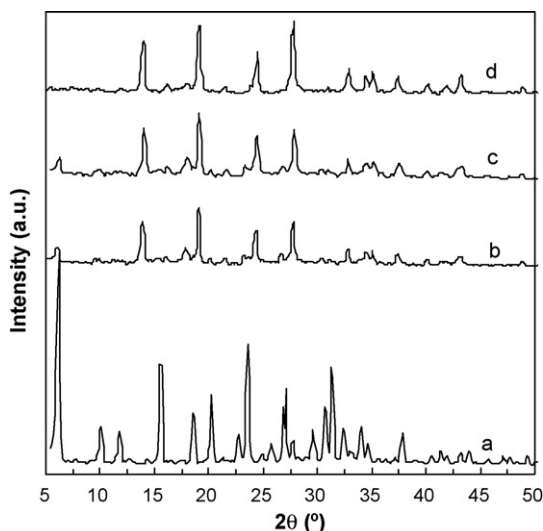


Fig. 5. XRD patterns of samples crystallized from the dry-gel with a composition of $5\text{Na}_2\text{O}:\text{Al}_2\text{O}_3:5\text{SiO}_2$. (a) Standard Y (by HTC route), (b and c) CAN + Y (100–120 °C for 24 h) and (d) CAN (140 °C for 24 h).

(Fig. 6b) and 16 (Fig. 6c) and Y zeolite (Fig. 6a) synthesized from a hydrogel of $5.5\text{Na}_2\text{O}:\text{Al}_2\text{O}_3:10\text{SiO}_2:180\text{H}_2\text{O}$ by an HTC route. Obviously, from the system of entry 16 with 2.0 of the $\text{H}_2\text{O}/\text{SiO}_2$ ratio one pure Y zeolite (typical of FAU topology) was successfully crystallized with some diffractions of 6.12° , 10.08° , 11.8° , 15.56° , 18.74° , 20.42° , 23.72° , 27.03° , 29.70° , 30.72° , 31.35° , 32.51° , 33.90° and 37.81° 2θ . The relative crystallinity and BET surface area of the calcined Y zeolite product ($\text{SiO}_2/\text{Al}_2\text{O}_3 = 4.5$) were measured to be 80% and $822.4 \text{ m}^2/\text{g}$. However, entry 15 with 1.33 of the $\text{H}_2\text{O}/\text{SiO}_2$ ratio resulted in only an unknown phase without the formation of Y phase. Hence, the effect of water amount in the dry-gel on the crystallization of Y zeolite by the DGC route was relatively profound. IR vibrations of Y framework emerged at 1116 , 986 , 770 , 692 , 573 and 474 cm^{-1} , where the peak at 573 cm^{-1} is the characteristic vibration of FAU zeolite.

TEM images of Y zeolites crystallized by different routes are displayed in Fig. 7. Distinctly, the morphology of Y zeolite prepared by the HTC route was constituted of large spherical crystallites with the size of 250–400 nm; however, that synthesized by the DGC route was consisted of spherical ultrafine particles with the size of 120–200 nm.

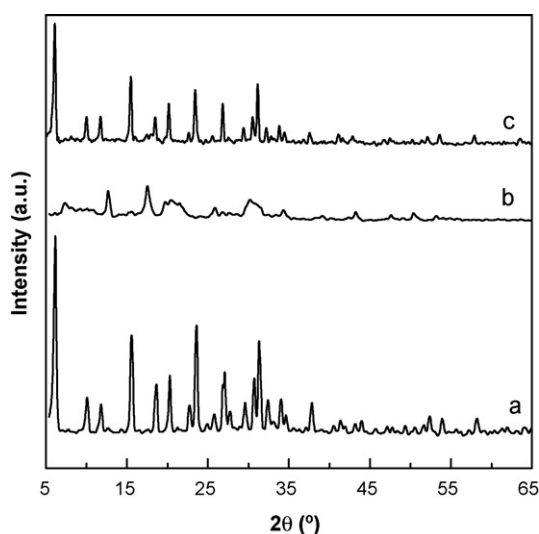


Fig. 6. Effect of the $\text{H}_2\text{O}/\text{SiO}_2$ ratio in the dry-gel on the DGC crystallization of Y zeolite with a composition of $5\text{Na}_2\text{O}:\text{Al}_2\text{O}_3:5\text{SiO}_2$. (a) Standard Y (by HTC route), (b) unknown (0.89) and (c) Y (1.33).

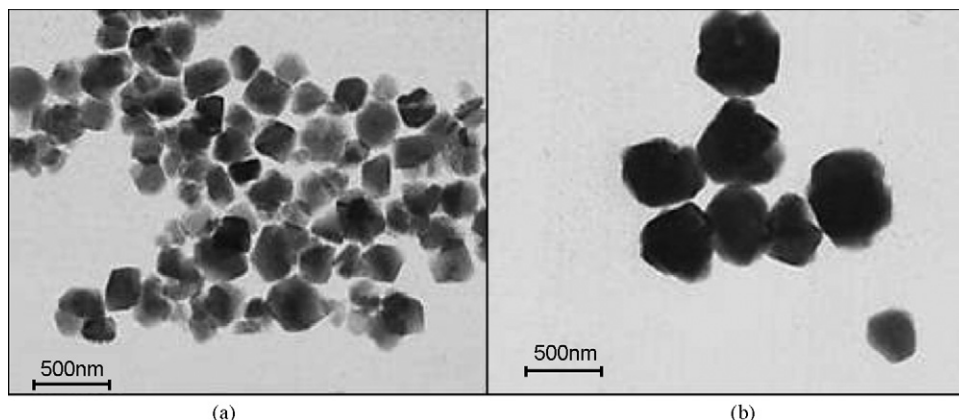


Fig. 7. TEM images of Y zeolites synthesized. (a) By DGC route at 50/90 °C and (b) by HTC route at 100 °C.

Comparatively, the DGC route could effectively control the crystal size of zeolites due to a different mass transfer from the HTC route. The steam resulting from the evaporation of water at the bottom assisted the complete crystallization of all dry-gel powder, while trace amount of water contained in the dry-gel notably limited the size of crystals in the range of ultrafine crystallites.

4. Conclusions

ZSM-5, mordenite, cancrinite and Y zeolites were successfully crystallized by the DGC without any organic additive (or template), in which the crystal particles of ZSM-5, mordenite and Y zeolite were controlled in the range of ultrafine size. The effects of crystallization conditions like reaction time, reaction temperature, water amount, $\text{SiO}_2/\text{Al}_2\text{O}_3$ and $\text{Na}_2\text{O}/\text{SiO}_2$ molar ratios were further investigated. With a molar ratio of $\text{SiO}_2/\text{Al}_2\text{O}_3 \leq 40$, the pure ZSM-5 zeolite was obtained at the $\text{Na}_2\text{O}/\text{SiO}_2$ molar ratio < 0.2 , but the pure mordenite was formed at the $\text{Na}_2\text{O}/\text{SiO}_2$ molar ratio > 0.25 . When the dry-gel with a composition of $5.0\text{Na}_2\text{O}:\text{Al}_2\text{O}_3:5.0\text{SiO}_2$ was crystallized at 140 °C for 24 h, pure CAN phase was obtained. Outstandingly, the DGC route effectively controlled the crystal size of zeolites due to a different mass transfer from the HTC route. TEM images showed that thus-crystallized zeolites consisted of ultrafine particles ranging 35–150 nm for ZSM-5, 50–200 nm for mordenite and 120–200 nm for zeolite Y, respectively. Different from ZSM-5, mordenite and cancrinite zeolites, the DGC crystallization of Y zeolite required more water in the dry-gel before crystallization, e.g. the suitable $\text{H}_2\text{O}/\text{SiO}_2$ molar ratio in the dry-gel was ca. 2.0, whereas the dry-gel with 1.33 of the $\text{H}_2\text{O}/\text{SiO}_2$ molar ratio converted to an unknown phase. This provides a new methodology for the synthesis of traditional zeolites with small crystals and low cost without any organic additive.

Acknowledgements

The authors thank the financial supports provided by National Natural Science Foundation of China (no. 20673035), by Dalian Institute of Chemical Physics of Chinese Academy of Sciences, and by the excellent mid-youth innovative team project of the Education Department of Hubei Province, China (no. T200701).

References

- [1] H. de St. Claire Deville, *Compt. Rend.* 54 (1862) 324.
- [2] W. Xu, J. Dong, J. Li, F. Wu, *J. Chem. Soc., Chem. Commun.* (1990) 755.
- [3] M. Matsukata, M. Ogura, T. Osaki, *Top. Catal.* 9 (1999) 77–92.
- [4] I. Schmidt, C. Madsen, C.J.H. Jacobsen, *Inorg. Chem.* 39 (2000) 2279.
- [5] (a) L. Tosheva, V.P. Valtchev, *Chem. Mater.* 17 (2005) 2494;
(b) S. Mintova, V.P. Valtchev, *Stud. Surf. Sci. Catal.* 125 (1999) 141.
- [6] G. Zhu, S. Qiu, J. Yu, Y. Sakamoto, F. Xiao, R. Xu, O. Terasaki, *Chem. Mater.* 10 (1998) 1483.
- [7] S.-Y. Sang, Z.-M. Liu, P. Tian, Z.-Y. Liu, L. Qu, Y. Zhang, *Mater. Lett.* 60 (2006) 1131.

- [8] T. Selvam, W. Schwieger, *Stud. Surf. Sci. Catal.* 142A (2002) 407.
- [9] B.O. Hincapie, L.J. Garces, Q. Zhang, A. Sacco, S.L. Suib, *Micropor. Mesopor. Mater.* 67 (2004) 19.
- [10] Q.-H. Xia, T. Tatsumi, *Mater. Chem. Phys.* 89 (2005) 89.
- [11] (a) Q. Li, D. Creaser, J. Sterte, *Micropor. Mesopor. Mater.* 31 (1999) 141;
(b) Q. Li, B. Mihailova, D. Creaser, J. Sterte, *Micropor. Mesopor. Mater.* 40 (2000) 53.
- [12] O. Larlus, V. Valtchev, J. Patarin, A.C. Faust, B. Maquin, *Micropor. Mesopor. Mater.* 56 (2002) 175.
- [13] P.A. Jacobs, J.A. Martens, *Stud. Surf. Sci. Catal.* 33 (1987) 26.